NMR IN BIOMEDICINE
NMR Biomed. 2006; **19**: 581–592
Published online 3 May 2006 in Wiley InterScience (www.interscience.wiley.com). DOI:10.1002/nbm.1038

Expression of transferrin receptor and ferritin following ferumoxides–protamine sulfate labeling of cells: implications for cellular magnetic resonance imaging†

Edyta Pawelczyk,[1]* Ali S. Arbab,[2] Sunil Pandit,[3] Elbert Hu[1] and Joseph A. Frank[1]

[1]Experimental Neuroimaging Section, Laboratory of Diagnostic Radiology Research, Clinical Center, National Institutes of Health, Bethesda, MD 20892, USA
[2]Department of Radiology, Henry Ford Health System, Detroit, MI 48202, USA
[3]Molecular Imaging Laboratory, Clinical Center, National Institutes of Health, Bethesda, MD 20892, USA

Received 28 October 2005; Revised 7 February 2006; Accepted 2 March 2006

ABSTRACT: Ferumoxides–protamine sulfate (FE-Pro) complexes are used for intracellular magnetic labeling of cells to non-invasively monitor cell trafficking by *in vivo* MRI. FE-Pro labeling is non-toxic to cells; however, the effects of FE-Pro labeling on cellular expression of transferrin receptor (TfR-1) and ferritin, proteins involved in iron transport and storage, has not been reported. FE-Pro-labeled human mesenchymal stem cells (MSCs), HeLa cells and primary macrophages were cultured from 1 week to 2 months and evaluated for TfR-1 and ferritin gene expression by RT-PCR and protein levels were determined using Western blots. MTT (proliferation assay) and reactive oxygen species (ROS) analysis were performed. FE-Pro labeling of HeLa and MSCs resulted in a transient decrease in TfR-1 mRNA and protein levels. In contrast, Fe-Pro labeling of primary macrophages resulted in an increase in TfR-1 mRNA but not in TfR-1 protein levels. Ferritin mRNA and protein levels increased transiently in labeled HeLa and macrophages but were sustained in MSCs. No changes in MTT and ROS analysis were noted. In conclusion, FE-Pro labeling elicited physiological changes of iron metabolism or storage, validating the safety of this procedure for cellular tracking by MRI. Published in 2006 by John Wiley & Sons, Ltd.

KEYWORDS: transferrin receptor (TfR-1); ferritin; mesenchymal stem cells; primary macrophages; cell labeling; SPIO; ferumoxides; protamine sulfate

INTRODUCTION

Ferumoxides is a dextran-coated superparamagnetic iron oxide nanoparticle (SPIO), Food and Drug Administration-approved magnetic resonance imaging (MRI) contrast agent used for hepatic imaging (1,2) and has been used to label phagocytic and non-phagocytic cells for *in vivo* cellular MRI (3–11). Following intravenous injection, ferumoxides accumulates in the Kupffer cells in the liver and in the reticuloendothelial system of the spleen (1,2). Ferumoxides is biodegradable and the iron is introduced into the normal plasma iron pool and can be incorporated into hemoglobin in erythrocytes or used for other metabolic processes (12).

A variety of methods have been developed to incorporate superparamagnetic iron oxide nanoparticles into cells (3,6,13–18). Coupling transfection agents to ferumoxides through electrostatic interactions facilitates the uptake of the SPIO nanoparticles into endosomes in cells (19). The potential of translating the ferumoxides–transfection agent labeling technique to clinical trials has been made possible by using a Food and Drug Administration-approved transfection agent, protamine sulfate complexed to ferumoxides for efficient labeling of stem cells, cancer and immune cells (7). Protamine sulfate has a molecular weight of approximately 4.2 kDa and is clinically used to reverse heparin-induced anticoagulation. Ferumoxides–protamine sulfate complexes (FE-Pro) used to label cells have no short- or long-term toxic effects, do not produce reactive oxygen species (ROS), do not modify viability and proliferation and do not alter cellular function, differentiation capacity or phenotype compared with unlabeled cells (7,20). However, the long-term fate of internalized iron oxide

**Correspondence to*: E. Pawelczyk, Experimental Neuroimaging Section, Laboratory of Diagnostic Radiology Research, Clinical Center, National Institutes of Health, Bethesda, MD 20892, USA. E-mail: pawelczyke@cc.nih.gov
Contract/grant sponsor: Intramural Research Program, Clinical Center, National Institutes of Health.

Abbreviations used: FE-Pro, ferumoxides–protamine sulfate complexes; HeLa, human cervical carcinoma cells; MCSs, mesenchymal stem cells; MTT, 3-(4,5-dimethylthiazol-2-yl)-2,5-diphenyltetrazolium bromide; PBS, phosphate-buffered saline; Pro, protamine sulfate; ROS, reactive oxygen species; RT-PCR, reverse transcriptase polymerase chain reaction; SDS-PAGE, sodium dodecyl sulfate polyacrylamide gel electrophoresis; SPIO, superparamagnetic iron oxide nanoparticle; TfR-1, transferrin receptor 1.

nanoparticles in endosomes and their effect on iron metabolic pathways in the cell have not been clearly elucidated (21).

The major route for cellular iron uptake involves receptor-mediated endocytosis of iron (Fe^{III})-loaded transferrins (22). Acidification of endosomes to $pH < 5.5$ leads to release of iron from transferrin and transport across the endosomal membrane by the divalent metal transporter. Internalized iron is utilized for metabolic purposes and excess is detoxified by sequestration into ferritin (22). Intracellular iron homeostasis is a tightly regulated balance between synthesis of iron storage protein – ferritin – and the synthesis of transferrin receptor, a molecule responsible for cellular iron uptake (23,24). When there is an increase in cytoplasmic iron content, ferritin synthesis is induced, resulting in sequestration of toxic iron (Fe^{II}) into the ferritin molecules (25). It is not known whether FE-Pro labeling alters cellular iron homeostasis.

Cellular uptake of FE-Pro complexes is probably by fluid phase endocytosis or macropinocytosis. Once internalized, iron oxide particles remain transiently in the endosome/lysosome compartment and can be visualized by Prussian blue staining (16,26,27). In rapidly dividing cells, intracellular iron can no longer be detected in cells following 5–8 divisions (26). In contrast, in slowly dividing or non-dividing cells such as mesenchymal stem cells grown to confluence, iron particles can be detected for more than 6 weeks (5). Recently, Arbab *et al.* showed that lysosomal pH of 4.5 dissolves iron oxide particles (27) that could lead to release of some of the iron (Fe^{II}) into the cytoplasm if it is not chelated to buffers. Since it is possible that labeled cells may contain superparamagnetic iron oxide nanoparticles for long periods of time, it is necessary to determine if the iron can be released from the endosome/lysosome compartment and become available to the metabolic pathways.

The objective of this study was to determine whether FE-Pro labeling alters *in vitro* gene and protein expression of transferrin receptor and ferritin, molecules involved in cellular iron transport and storage over time and to elucidate how cell labeling affects proliferation, production of ROS and differentiation in MSC, HeLa cells and primary macrophages.

METHODS

Cell culture and labeling

Human mesenchymal stem cells (MSCs) (Cambrex Bio Science Walkersville, Walkersville, MD, USA) and human cervical carcinoma (HeLa) (CCL-2, ATCC, Manassas, VA, USA) grown in standard culture media at 37 °C and in a 95% air per 5% CO_2 atmosphere were used. Cells were allowed to grow until 90% confluence in 75-cm^2 culture flasks prior to labeling. Primary monocytes, isolated from healthy donors and obtained from the NIH Blood Bank, were plated in 75-cm^2 culture flasks at a density of 10^7 cells/mL. Monocytes were cultured for 7 days in RPMI 1640 media (ATCC) with 10% fetal bovine serum (Atlanta Biologicals, Norcross, GA, USA) and granulocyte macrophage colony-stimulating factor (50 ng/mL, PeproTech, Rocky Hill, NJ, USA) to allow differentiation of monocytes into macrophages. The ferumoxides suspension (Feridex IV, Berlex Laboratories, Wayne, NJ, USA) is provided at a total iron content of 11.2 mg/mL. Protamine sulfate (Pro, American Pharmaceuticals Partner, Schaumburg, IL, USA), supplied at 10 mg/mL, was prepared as a fresh stock solution of 1 mg/mL in sterile distilled water immediately before labeling. Ferumoxides at a concentration of 100 μg/mL was placed in a 50-mL conical tube containing serum-free RPMI 1640 (Biosource, Camarillo, CA, USA) with 25 mM 4-(2-hydroxyethyl)-1-piperazinethanesulfonic acid, minimum essential medium, non-essential amino acids, sodium pyruvate and L-glutamine. Protamine sulfate was added to the solution at 6 μg/mL and mixed for 3 min with intermittent manual shaking. Culture medium was aspirated from the flasks and cells were overlaid with media containing FE-Pro. After 1 h of incubation with primary macrophages and 2 h of incubation with HeLa cells and MSCs, at 37 °C, an equal amount of relevant complete medium was added to HeLa and MSCs for a final concentration of FE to Pro of 50 μg/mL to 3 μg/mL. Primary macrophages were washed three times with sterile phosphate-buffered saline (PBS) containing 10 U/mL heparin sulfate (American Pharmaceuticals Partner, Schaumburg, IL, USA) to remove excess FE-Pro and cultured in complete medium for 7 days. HeLa cells and MSCs were incubated overnight (~16 h) and washed three times with sterile PBS containing 10 U/mL heparin sulfate (American Pharmaceuticals Partner). Complete medium was added to each flask and labeled cells unlabeled control cells were kept in culture for up to 28 days, with a change of medium every 4 days.

In addition, FE-Pro-labeled and unlabeled MSCs grown to 100% confluence were frequently divided over a period of 2 months. The first passage was performed 24 h after labeling, with subsequent division of the cells in the flasks at 1, 2, 4 and 9 weeks, corresponding to the second, third, fourth and seventh passage post-labeling.

For this study, MSCs were chosen as a primary stem cell line that can proliferate without differentiating in culture. HeLa cells were used as rapidly dividing cells and have been used in our previous studies (26). Primary macrophages are professional phagocytes involved in professional removal of cellular debris in areas of inflammation and could incorporate iron from extracellular space. Activated macrophages derived from circulating monocytes were used because of their short lifespan *ex vivo* and therefore would serve for comparison with other MSC and HeLa cells.

Histology and labeling efficiency

At each time point (i.e. days 1, 3, 7, 14, 21 and 28), cells were trypsinized and transferred to cytospin slides. Cells were fixed with 4% glutaraldehyde, washed and incubated for 30 min with 2% potassium ferric ferrocyanide (Perl's reagent for Prussian blue staining, Sigma, St. Louis, MO, USA) in 3.7% hydrochloric acid. Cells were washed again, counterstained with nuclear fast red and evaluated for iron staining with a Zeiss microscope (Axioplan Imaging II; Zeiss, Oberkochen, Germany) at ×40/0.75 objective lens and Axiovision 4 software (Zeiss). The images were processed using Adobe Photoshop 7.0 (Adobe, San Jose, CA, USA).

FE-Pro labeling efficiency was determined by manual counting of Prussian blue-stained and unstained cells using a Zeiss microscope (Axioplan Imaging II) at ×100 magnification using a ×100/1.30 (oil) immersion objective lens. The percentage of labeled cells was determined from the average of five high-powered fields.

Real-time quantitative RT-PCR analysis

In order to assess the expression levels of genes encoding transferrin receptor 1 (TfR-1) and ferritin, total RNA was isolated from 2×10^6 labeled and unlabeled control MSCs, HeLa cells and primary macrophages at day 1 through day 28 post-labeling, using an RNeasy Mini Kit (Qiagen, Valencia, CA, USA). For each RNA sample, 1 μg was used as a template for first-strand cDNA synthesis using a TaqMan High Capacity cDNA Archive Kit, following the RT-PCR manufacturer's two-step protocol (PE Applied Biosystems, Foster City, CA, USA). Controls included RNA samples without reverse transcriptase and no RNA with reverse transcriptase. Quantitative analysis of TfR-1 and ferritin gene was performed by real-time quantitative PCR using ABI Prism 7700 Sequence Detection System (PE Applied Biosystems) with TaqMan chemistries and probes. The TaqMan probes and primers for target genes were assay on demand gene expression products (PE Applied Biosystems). The following validated PCR primers and TaqMan MGB probes (FAM labeled) were used: human TfR-1 (assay ID: Hs66666611_m1), human ferritin (assay ID: Hs01694011_s1) and 18S ribosomal RNA (assay ID: 4333760F) as endogenous control (PE Applied Biosystems). Optimal primer, probe and cDNA concentrations were determined in a separate set of experiments to ensure that both target gene and 18S RNA fragments were amplified with equal efficiency. PCR reactions were performed with first-strand cDNA (0.5 μL for TfR-1 and 1 μL for ferritin) from each sample, a Universal PCR Master Mix kit (PE Applied Biosystems), 250 nM TaqMan probe, 0.16 U of AmpErase UNG (uracil-*N*-glycosylase) and 900 nM forward–reverse primers of each gene and 18S RNA. Three measurements per sample were performed in each of two independent experiments. Results were analyzed with the ABI Sequence Detector software version 1.7 (PE Applied Biosystems). For relative quantification of target gene expression, the calibration curve method was applied. Calibration curves were generated by serially diluting universal human reference cDNA (Stratagene, La Jolla, CA, USA). The normalized target gene value was determined by dividing the average target gene value by the average 18S RNA value. The normalized target gene value is unitless and is used for comparing the relative amounts of target gene in different samples.

Western blot analysis

Cell pellets collected at each time point were lysed with CelLytic-M (Sigma). Lysates were cleared by centrifugation at 14 000 *g* for 15 min. Protein concentration was measured using a BCA Protein Assay (Pierce, Rockford, IL, USA). Aliquots of lysates containing 30 or 40 μg total protein were incubated with Laemmli buffer (28) for 5 min at 95 °C and were subjected to reducing sodium dodecyl sulfate polyacrylamide gel electrophoresis (SDS-PAGE) on 10% gels for analysis of TfR-1 or 12% gels for analysis of ferritin. Protein was transferred to nitrocellulose and was detected using mouse anti-hTfR-1 (1:1000) (Alpha Diagnostic, San Antonio, TX, USA), rabbit polyclonal anti-human ferritin, detecting both light and heavy subunits (1:1000) (Abcam, Cambridge, MA, USA), mouse anti-hβ-actin (1:1000) (Sigma) or rabbit-anti-hβ-actin (1:1000) (Sigma) antibodies and then horseradish peroxidase (HRP)-conjugated (1:2000) secondary antibodies. Bands were visualized by chemiluminescence (ECL Plus Western Blotting Reagent, Amersham Biosciences, Piscataway, NJ, USA), quantitated by spot densitometry using a Kodak Image Station 1000 (Eastman Kodak, Rochester, NY, USA) and normalized to β-actin.

Cell viability and proliferation/cytotoxicity after FE-Pro labeling of cells

The viability of FE-Pro-labeled MSCs, HeLa cells and primary macrophages was evaluated with 3-(4,5-dimethylthiazol-2-yl)-2,5-diphenyltetrazolium bromide (MTT) assay (Roche Molecular Biochemicals, Indianapolis, IN, USA) and trypan blue exclusion test. MTT assay is a colorimetric method for determining the number of viable cells in proliferation or serves as a cytotoxicity assay (29,30). It is based on the reduction of the yellow tetrazolium salt MTT to purple formazan crystals by metabolically active cells, in part by the action of dehydrogenase enzymes, to generate reducing equivalents such as NADH and NADPH, and therefore is a

reflection of mitochondrial function (31). The resulting intracellular purple formazan can be solubilized and quantified by spectrophotometric means. FE-Pro-labeled cells and unlabeled cells were grown in triplicate or quadruplicate in 96-well plates at 1×10^5 cells/well with a change of medium every 3 days. At each time point, MTT was added to the medium at a final concentration of 0.5 mg/mL and cells were incubated for 3 h at 37 °C in a 5% CO_2 atmosphere. After incubation, an equal volume of solubilizer buffer was added according to the manufacturer's instructions (Roche Molecular Biochemicals) and the cells were incubated overnight at 37 °C in a 5% CO_2 atmosphere. The absorbance of the formazen product was measured at a wavelength of 570 nm, with 750 nm as the subtracted reference wavelength.

Reactive oxygen species (ROS) measurements

The intracellular formation of ROS was detected by using a CM-H_2DCFDA fluorescent probe (Molecular Probes, Eugene, OR, USA), a non-fluorescent indicator that forms fluorescent esters when it reacts with ROS inside cells. FE-Pro-labeled cells and unlabeled cells were grown in triplicate or quadruplicate for ROS analysis.

At each time point, 1×10^6 cells were suspended in PBS with a final concentration of CM-H_2DCFDA of 10 μM and incubated for 1 h at 37 °C in a 5% CO_2 atmosphere. Thereafter, cells were washed twice and resuspended in PBS. An increase in fluorescence was detected by flow cytometry (FACS Calibur, Becton Dickinson, Franklin Lakes, NJ, USA). A total of 10 000 cells were analyzed at the FL1 detector and the results were presented as mean geometric fluorescence.

Differentiation of MSC

To determine whether MSCs retained the ability to differentiate after labeling with FE-Pro, labeled and unlabeled control MSCs at week 1 and week 2 post-labeling were subjected to adipogenic and chondrogenic differentiation. For adipogenic assay, MSCs were plated on 35-cm^2 culture dishes and cultured until they reached 100% confluence. The stimulation of adipogenic differentiation was performed according to the cell supplier's instructions (Cambrex Bio Science Walkersville). Three alternate cycles of induction and maintenance were performed in a 3-week time period. After the third cycle, the medium was gently aspirated and cells were fixed in 10% buffered formalin and stained with Oil Red O. Only cells with neutral lipid vacuoles stained red. For the chondrogenic assay, 1 and 2 weeks after labeling, cells were trypsinized, washed and gently centrifuged to form a pellet micromass, which was cultured in a chondrogenic differentiation media (Cambrex Bio Science Walkersville) for 21 days. Pellets were sectioned and stained with Safranin O to detect proteoglycans (7,32).

Determination of iron concentration per cell

The iron concentration inside the labeled cells was assessed using NMR relaxometry (33,34). In brief, pellets containing 1×10^6 cells were dried overnight at 110 °C and incubated for 3 h at 60 °C in a heating block in 500 μL of a mixture of perchloric acid and nitric acid (3:1). For completely digested samples, the NMR relaxation rate $1/T_2$ (s^{-1}) was measured at room temperature and 1.0 T using a custom-designed variable-field NMR relaxometer and a Carr–Purcell–Meiboom–Gill pulse sequence (33,34). The iron concentration in the samples was calculated from a calibration curve that was derived from calibration standards of ferrous chloride containing 0.01–10 mM iron in the same acid proportions. Iron content was expressed as an average in picograms of iron per cell.

Statistical analysis

Each experiment was performed at least twice and each sample was tested in triplicate or quadruplicate. Data are expressed as a mean ± SD. A statistically significant difference between FE-Pro-labeled cells and corresponding unlabeled cells was determined by a paired two-tailed Student's *t*-test or non-parametric statistics where data were not Gaussian distributed (Prism 4 for Macintosh; Graph Pad Software, San Diego, CA, USA). A value of $p < 0.05$ was considered significant.

RESULTS

FE-Pro labeling of HeLa, MSCs and primary macrophages

FE-Pro labeling of HeLa, MSCs and primary macrophages resulted in approximately 100% labeling efficiency after counting of Prussian blue-stained cells. Representative photomicrographs of Prussian blue stains of HeLa, MSCs and primary macrophages from day one revealed abundant uptake of the FE-Pro complex into the cytoplasm (Fig. 1) with no Prussian blue positive unlabeled HeLa, MSCs or macrophages. The labeling intensity and amount of iron per cell of slowly dividing MSCs were comparable at each time point investigated (Table 1). In contrast, in rapidly dividing HeLa cells or

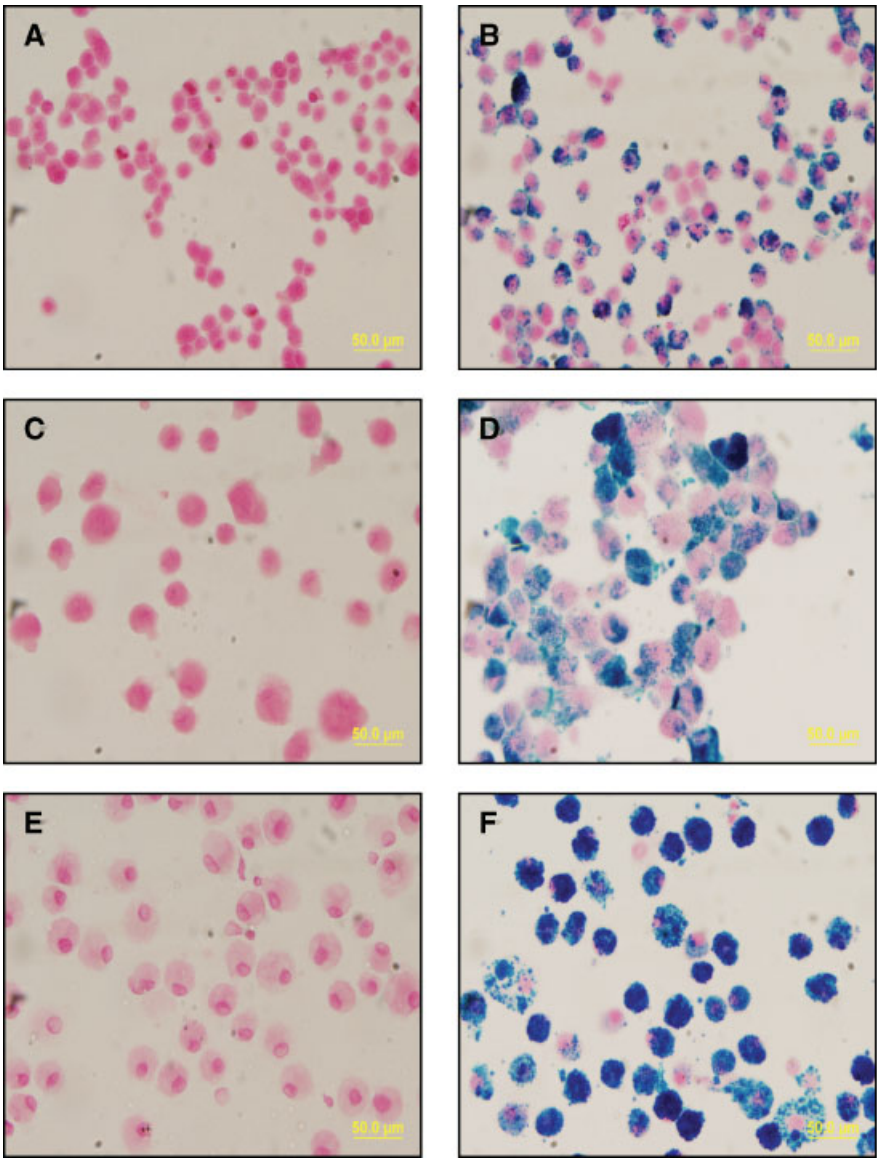

Figure 1. Representative Prussian blue photomicrographs (magnification × 40) of: unlabeled (A) and FE-Pro-labeled HeLa cells (B) 1 day after labeling; unlabeled (C) and FE-Pro-labeled MSCs (D) 1 day after labeling; and unlabeled (E) and Fe-Pro-labeled primary macrophages (F) 1 day after labeling

Table 1. Iron content, proliferation/cytotoxicity and ROS production in FE-Pro-labeled MSCs[a]

		Day 1	Day 3	Day 7	Day 14	Day 21	Day 28
Fe (pg/cell)	(L)	$44.7 \pm 0.34^{***}$	$24.8 \pm 0.29^{***}$	$16.5 \pm 0.78^{***}$	$37.5 \pm 0.81^{***}$	$41.2 \pm 0.71^{***}$	$57 \pm 0.56^{***}$
	(U)	(0.37 ± 0.36)	(0.22 ± 0.04)	(0.12 ± 0.02)	(0.16 ± 0.03)	(0.19 ± 0.03)	(0.32 ± 0.04)
MTT	(L)	0.56 ± 0.06	0.53 ± 0.04	0.62 ± 0.01	0.53 ± 0.04	0.67 ± 0.04	1.01 ± 0.08
	(U)	(0.45 ± 0.09)	(0.44 ± 0.02)	(0.47 ± 0.006)	(0.44 ± 0.01)	(0.45 ± 0.05)	(0.91 ± 0.06)
ROS	(L)	75.1 ± 9.4	164.7 ± 11	186.5 ± 9.5	424.8 ± 27.4	431.7 ± 2.4	441.9 ± 2.7
	(U)	(98.5 ± 6.4)	(138 ± 14.9)	(170.1 ± 16.2)	(426.5 ± 4.9)	(443.7 ± 5.3)	(419.7 ± 0.4)

[a]Data are presented as a mean ± 1 SD from three samples. Statistical analysis was performed by comparing iron content (picograms per cell), MTT and ROS production in FE-Pro-labeled (L) cells with corresponding unlabeled (U) cells presented in parentheses. $^{***}p < 0.0001$.

non-dividing macrophages, with time, there was a decrease in labeling intensity and iron content owing to cell division, potential cellular iron metabolism or transport of nanoparticles back out into extracellular space (Tables 2 and 3).

TfR-1 and ferritin levels in FE-Pro-labeled HeLa cells

Rapidly dividing Fe-Pro-labeled HeLa cells that were maintained in culture for 28 days, demonstrated a

Table 2. Iron content, proliferation/cytotoxicity and ROS production in FE-Pro-labeled HeLa cells[a]

		Day 1	Day 3	Day 7	Day 14	Day 21	Day 28
Fe (pg/cell)	(L)	$18.86 \pm 0.32^{***}$	$5.99 \pm 1.91^{*}$	$5.25 \pm 1.38^{*}$	$5.19 \pm 1.88^{*}$	4.71 ± 2.48	$2.33 \pm 0.15^{**}$
	(U)	(0.28 ± 0.07)	(0.12 ± 0.02)	(0.16 ± 0.02)	(0.15 ± 0.04)	(0.24 ± 0.03)	(0.22 ± 0.04)
MTT	(L)	1.27 ± 0.04	1.29 ± 0.006	1.22 ± 0.05	1.08 ± 0.05	0.84 ± 0.04	0.83 ± 0.06
	(U)	(1.31 ± 0.08)	(1.30 ± 0.06)	(1.28 ± 0.05)	(0.90 ± 0.02)	(0.93 ± 0.05)	(0.90 ± 0.06)
ROS	(L)	1270 ± 107.3	469.4 ± 43.9	111.8 ± 14.27	243.1 ± 7.2	247.3 ± 16.9	270 ± 17.6
	(U)	(1216 ± 77.33)	(388.6 ± 30.0)	(123.6 ± 40.9)	(212.4 ± 19.2)	(212.1 ± 32.74)	(244 ± 10.3)

[a]Data are presented as a mean $\pm$ 1 SD from three samples. Statistical analysis was performed by comparing iron content (picograms per cell), MTT and ROS production in FE-Pro labeled (L) cells with corresponding unlabeled (U) cells presented in parentheses. $^{*}p < 0.04$; $^{**}p < 0.001$; $^{***}p < 0.0001$.

Table 3. Iron content, proliferation/cytotoxicity and ROS production in FE-Pro-labeled primary macrophages[a]

		Day 1	Day 3	Day 7
Fe (pg/cell)	(L)	$22.7 \pm 1.13^{**}$	$23.7 \pm 0.92^{***}$	$11.2 \pm 1.51^{*}$
	(U)	(0.6 ± 0.57)	(0.37 ± 0.19)	(1.38 ± 0.66)
MTT	(L)	0.21 ± 0.03	0.31 ± 0.01	0.37 ± 0.01
	(U)	(0.18 ± 0.02)	(0.30 ± 0.006)	(0.34 ± 0.03)
ROS	(L)	492.3 ± 25.8	123.1 ± 22.3	325.0 ± 45.1
	(U)	(544.1 ± 13.1)	(128.9 ± 25.9)	(337.5 ± 67.1)

[a]Data are presented as a mean $\pm$ 1 SD from three samples. Statistical analysis was performed by comparing iron content (picograms per cell), MTT and ROS production in FE-Pro labeled (L) cells with corresponding unlabeled (U) cells presented in parentheses. $^{*}p < 0.02$; $^{**}p < 0.001$; $^{***}p < 0.0006$.

decreasing trend in TfR-1 mRNA expression with time [Fig. 2(A)]. A significant decrease in TfR-1 transcript levels was detected only at early time points between days 1 and 7 ($p < 0.007$) [Fig. 2(A)]. TfR-1 protein expression levels correlated with TfR-1 gene expression transcripts and the protein levels were decreased at most of the time points [Fig. 2(B)]. A significantly lower TfR-1 protein expression was obtained from the whole cell lysate of labeled HeLa cells on days 3 ($p = 0.012$) and 7 ($p = 0.023$) when compared with lysate from unlabeled HeLa cells [Fig. 2(B)]. In contrast, ferritin gene transcripts were slightly increased in labeled HeLa cells as early as at day 1, although the difference was not significant compared with unlabeled cells [Fig. 2(C)]. An increasing trend in ferritin gene transcripts was observed on days 7, 14, 21 and 28 with a significant increase in ferritin mRNA levels from labeled HeLa cells detected only on day 7 ($p = 0.002$), compared with unlabeled cells [Fig. 2(C)]. Ferritin protein levels from whole HeLa lysate were higher compared with ferritin levels of corresponding controls during the first two weeks after labeling, on days 1 ($p = 0.04$), 3 ($p = 0.002$), 7 ($p = 0.033$) and 14 ($p = 0.002$) [Fig. 2(D)]. At days 21 and 28, there was no significant difference detected in the levels of ferritin protein between labeled and unlabeled HeLa cell lysate.

TfR-1 and in ferritin levels of FE-Pro-labeled MSCs

FE-Pro labeling of MSCs grown to confluence for 28 days resulted in a significant decrease of TfR-1 mRNA expression as early as 24 h ($p = 0.006$), 3 days ($p = 0.012$), 7 days ($p = 0.005$) and 14 days ($p = 0.009$) after labeling compared with unlabeled MSCs [Fig. 3(A)]. At other time points, lower TfR-1 transcript levels were detected compared with unlabeled cells, but the differences were not significant. TfR-1 protein expression from labeled MSCs lysate were found with decreased levels on days 3, 7 and 28 but were unchanged compared to control cells on days 1, 14 and 21 [Fig. 3(B)]. A significant decrease in TfR-1 protein expression from labeled MSCs was detected on days 3 ($p = 0.004$) and 7 ($p = 0.003$) [Fig. 3(B)].

In general, ferritin expression from FE-Pro-labeled mesenchymal stem cells grown to confluence demonstrated an insignificant increase in ferritin mRNA expression compared with corresponding unlabeled cells in culture [Fig. 3(C)]. A significant increase in ferritin mRNA was only observed on days 14 ($p = 0.025$) and 28 ($p = 0.009$) [Fig. 3(C)]. However, the ferritin protein levels were significantly increased at each time point ($p < 0.002$) compared with unlabeled MSCs whole cell lysate [Fig. 3(D)].

TfR-1 and ferritin protein levels were also determined for FE-Pro-labeled and unlabeled MSCs that were allowed to slowly proliferate by serially dividing the cell cultures in half , when they reached confluence thus diluting iron content per cell (Fig. 4). Multiple passages of labeled MSCs resulted in a significant decrease in TfR-1 protein observed only at passage 1 (24 h after labeling, $p = 0.040$) and not significantly different but lower TfR-1 protein levels at passages 2 and 3 compared with unlabeled MSCs [Fig. 4(A)]. By passage 4, TfR-1 protein levels of FE-Pro labeled MSC were similar to unlabeled MSCs or slightly higher [Fig. 4(A)]. In comparison, ferritin protein levels from labeled MSCs were significantly increased after passages 1 ($p = 0.007$), 3 ($p < 0.0001$) and 4 ($p = 0.0023$) compared with unlabeled cells [Fig. 4(B)]. After seven passages or week 9 in culture, ferritin levels from Fe-Pro-labeled cells were not significantly increased compared with unlabeled cells.

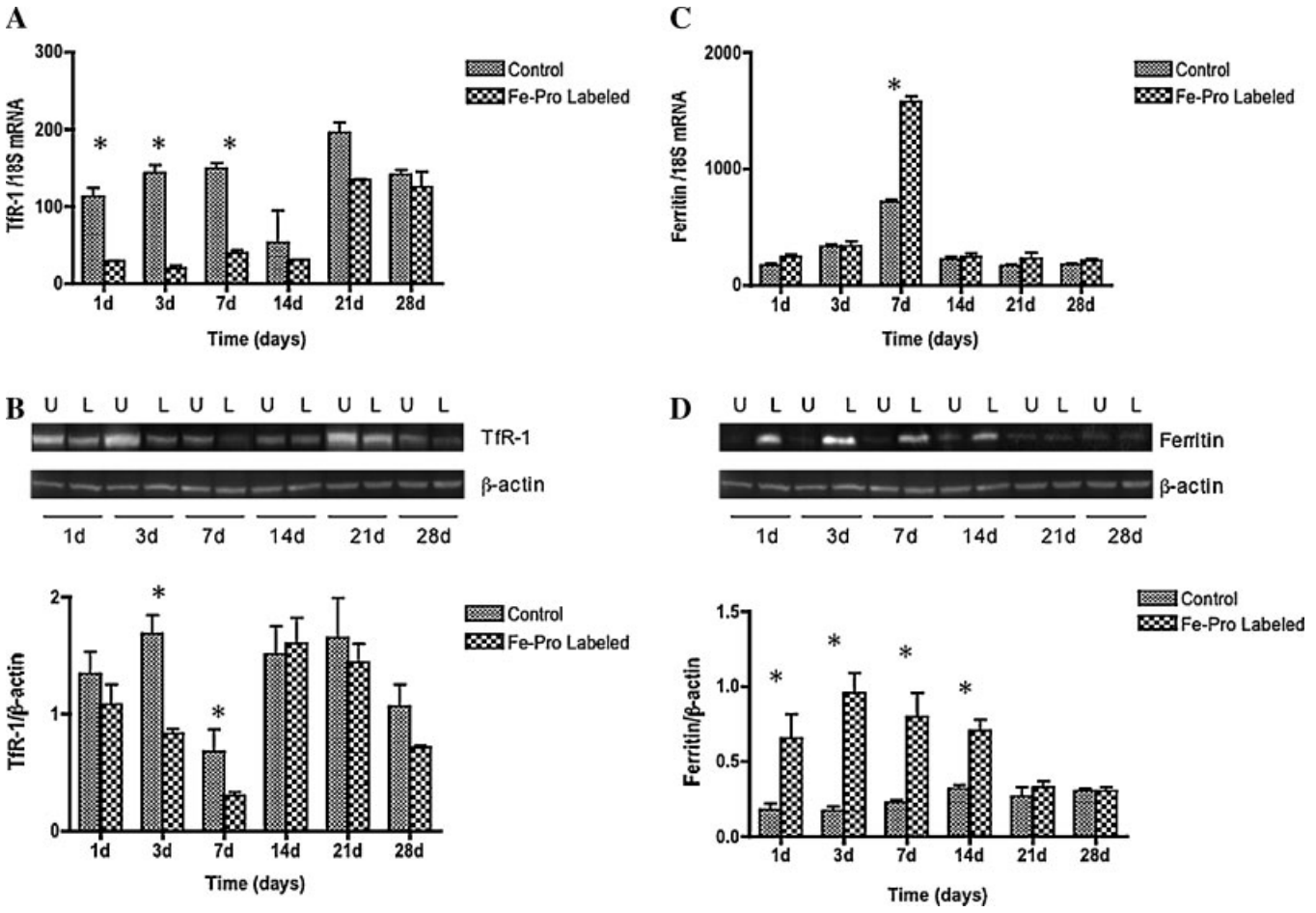

Figure 2. TfR-1 and ferritin gene and protein expression in FE-Pro-labeled HeLa cells 1–28 days post-labeling determined by real-time RT-PCR and Western blotting of whole cell lysate. (A, C) Decreases in TfR-1 gene expression in labeled HeLa cells on days 1 ($p = 0.007$), 3 ($p = 0.004$) and 7 ($p < 0.001$) and increase in ferritin gene expression on day 7 ($p = 0.002$) compared with corresponding unlabeled cells. Results are expressed as a relative TfR-1 or ferritin mRNA expression normalized to 18S RNA (mean ± 1 SD). (B, D) Representative Western blots of TfR-1 and ferritin protein levels, quantitated and presented on graphs below. Note the decrease in TfR-1 protein levels on days 3 ($p = 0.012$) and 7 ($p = 0.023$) and increase in ferritin protein expression in labeled cells (L) on days 1 ($p = 0.04$), 3 ($p = 0.002$), 7 ($p = 0.033$) and 14 ($p = 0.002$) compared with corresponding unlabeled cells (U). Results are expressed as relative TfR-1 or ferritin protein expression normalized to β-actin (mean ± 1 SD). * = Significant differences from the control

TfR-1 and ferritin levels of FE-Pro-labeled primary macrophages

Matured primary macrophages that were maintained in culture for 7 days after Fe-Pro labeling demonstrated increased expression of TfR-1 mRNA at days 1 ($p = 0.0006$), 3 ($p = 0.0007$) and 7 ($p = 0.0189$) [Fig. 5(A)]. However, no significant changes in TfR-1 expression at the protein level were detected between labeled and unlabeled macrophages at any time point analyzed [Fig. 5(B)]. Ferritin gene expression in Fe-Pro-labeled macrophages was significantly increased at days 1 ($p = 0.045$), 3 ($p = 0.0115$) and 7 ($p = 0.0005$) compared with unlabeled cells [Fig. 5(C)]. Ferritin protein levels were higher in labeled macrophages on days 1 ($p = 0.0122$) and 7 ($p = 0.0326$) [Fig. 5(D)].

Cellular viability, proliferation/cytotoxicity and ROS production after FE-Pro labeling

Tables 1–3 contain the results of the MTT (i.e. proliferation/cytotoxicity assay) and ROS analysis measured at different time intervals from days 1–28 for FE-Pro-labeled and unlabeled HeLa, MSCs and macrophages. In HeLa cells, there was a decreasing trend in formazen (MTT assay product) production over time in both labeled and unlabeled cells, whereas for MSCs formazen production was comparable at each time point. Labeled macrophages showed an increasing trend in formazen production over time compared with unlabeled cells. No significant decrease in the viability by trypan blue exclusion or proliferation of the labeled MSCs, HeLa cells or macrophages were observed at all time points

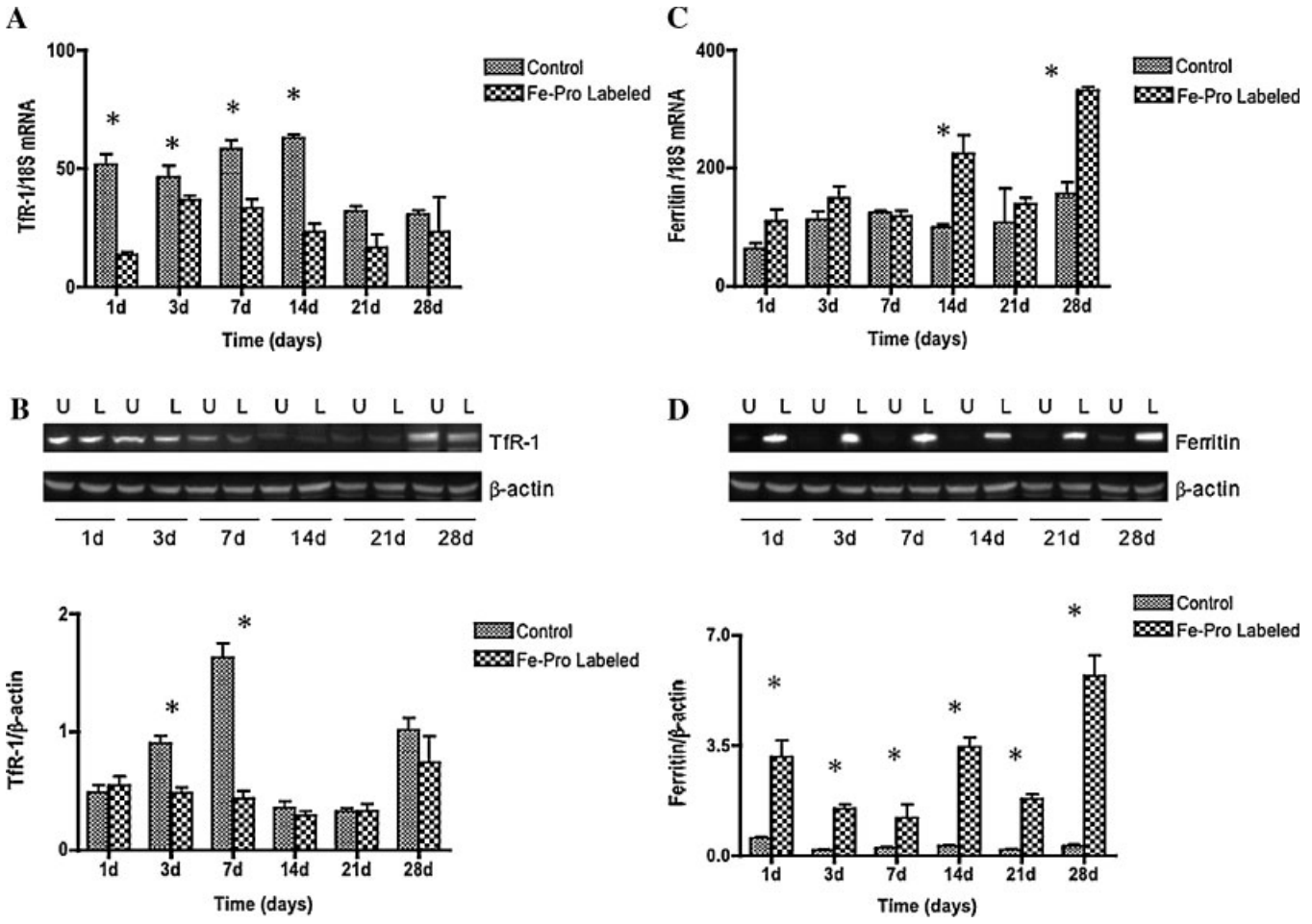

Figure 3. TfR-1 and ferritin gene and protein expression in FE-Pro-labeled MSCs 1–28 days post-labeling determined by real-time RT-PCR and Western blots of whole cell lysate. (A, C) Decrease in TfR-1 gene expression in labeled MSCs on days 1 ($p = 0.006$), 3 ($p = 0.012$), 7 ($p = 0.005$) and 14 ($p = 0.01$) and increase in ferritin gene expression on days 14 ($p = 0.025$) and 28 ($p = 0.009$) compared with corresponding unlabeled cells. Results are expressed as a relative TfR-1 or ferritin mRNA expression normalized to 18S RNA (mean $\pm$ 1 SD). (B, D) Representative Western blots of TfR-1 and ferritin protein levels quantitated and presented on graphs below. Note the decreases in TfR-1 protein levels in labeled cells (L) on days 3 ($p = 0.004$) and 7 ($p = 0.003$) and increases in ferritin protein expression on days 1 ($p = 0.002$), 3 ($p = 0.0003$), 7 ($p = 0.021$), 14 ($p = 0.0002$), 21 ($p = 0.0001$) and 28 ($p = 0.001$) compared with corresponding unlabeled cells (U). Results are expressed as relative TfR-1 or ferritin protein expression normalized to β-actin (mean $\pm$ 1 SD). * = Significant differences from the controls

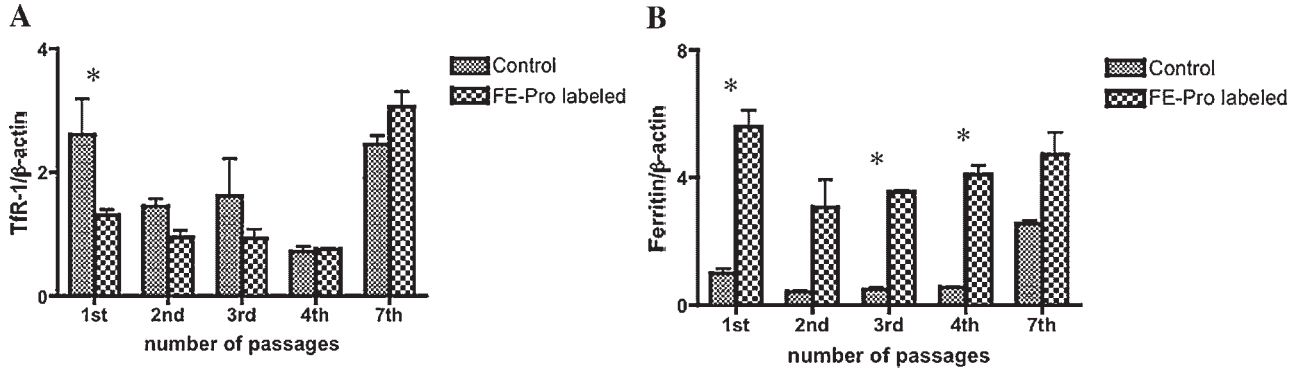

Figure 4. TfR-1 and ferritin protein expression in FE-Pro-labeled MSCs after serially passing cells for over 2 months. (A) A significant decrease in TfR-1 protein levels is noted after passage 1 ($p = 0.04$) but not after passages 2–7 compared with unlabeled cells. (B) Increase in ferritin protein levels after passages 1 ($p = 0.007$), 2 ($p = 0.094$), 3 ($p < 0.0001$) and 4 ($p = 0.002$) compared with corresponding unlabeled cells. Results are expressed as relative TfR-1 or ferritin protein expression normalized to β-actin (mean $\pm$ 1 SD). * = Significant difference from the controls

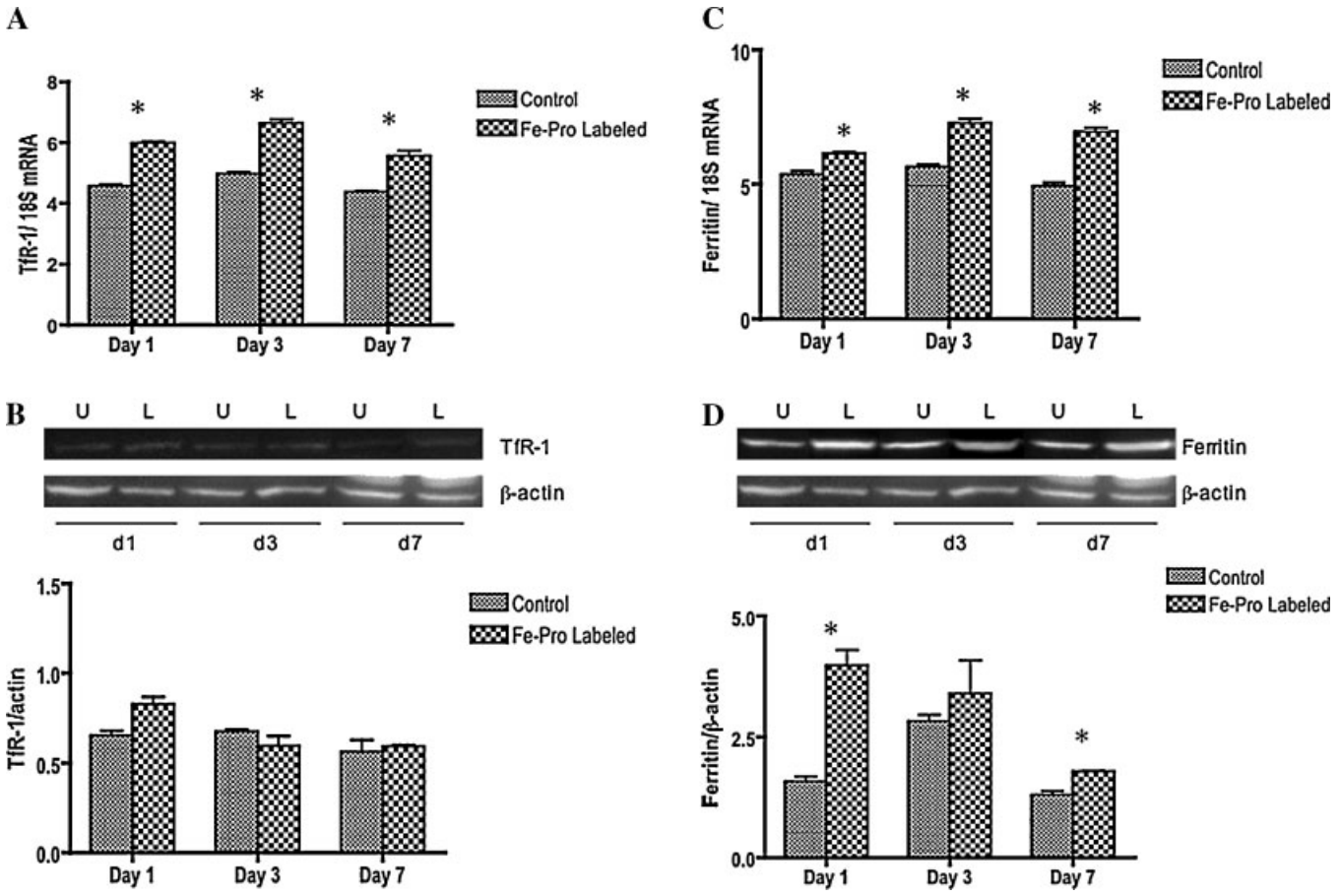

Figure 5. TfR-1 and ferritin gene and protein expression in FE-Pro-labeled primary macrophages 1–7 days post-labeling determined by real-time RT-PCR and Western blots of whole cell lysate. (A, C) Increase in TfR-1 gene expression in labeled macrophages on days 1 ($p = 0.0006$), 3 ($p = 0.0007$) and 7 ($p = 0.019$) and increase in ferritin gene expression on days 1 ($p = 0.045$), 3 ($p = 0.0115$) and 7 ($p = 0.0005$) compared with corresponding unlabeled cells. Results are expressed as a relative TfR-1 or ferritin mRNA expression normalized to 18S RNA (mean ± 1 SD). (B, D) Representative Western blots of TfR-1 and ferritin protein levels, quantitated and presented on graphs below. Note no significant changes in TfR-1 protein levels and increases in ferritin protein expression in labeled cells (L) on days 1 ($p = 0.0122$) and 7 ($p = 0.0326$) compared with corresponding unlabeled cells (U). Results are expressed as relative TfR-1 or ferritin protein expression normalized to β-actin (mean ± 1 SD). * = Significant differences from the controls

compared with corresponding unlabeled cells (data not shown).

The ROS production values represented by the geometric mean fluorescence (Tables 1–3) were not significantly different in labeled MSCs and HeLa cells compared with the corresponding unlabeled cells. Fe-Pro labeling of primary macrophages demonstrated no significant changes in ROS production compared with unlabeled cells.

Effect of FE-Pro labeling on differentiation capacity of MSCs

Labeling of MSCs with FE-Pro complexes did not alter the capacity of MSCs to differentiate when grown in culture with appropriate growth factors. Both FE-Pro-labeled and unlabeled MSCs showed similar differentiation to adipogenic and chondrogenic lineages 1 week post-labeling (data not shown) and 2 weeks post-labeling (Fig. 6).

DISCUSSION

The major finding of the study of effects of labeling cells with FE-Pro on cellular iron metabolism is that the cells increased gene and protein expression of ferritin in response to ferumoxides loading into endosomes and at the same time down-regulated the gene and protein expression of the transferrin receptor.

Following labeling of cells with ferumoxides, the nanoparticles may remain inside the endosomes for an extended period of time or may circulate back out into extracellular space in rapidly dividing cells (7,26). A recent study from our laboratory has shown that some of

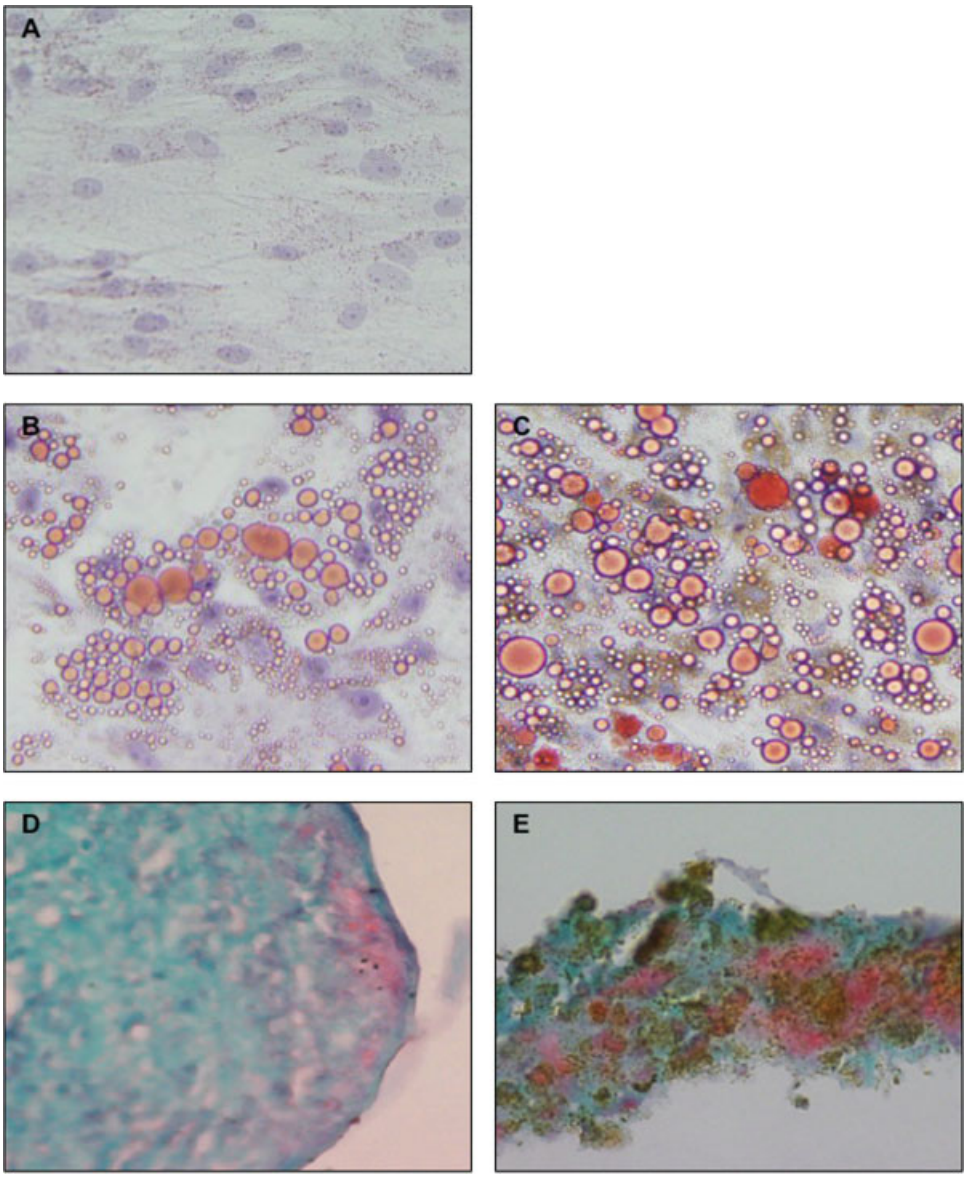

Figure 6. Differentiation of FE-Pro-labeled and unlabeled MSCs 2 weeks after labeling. (A) MSC-unlabeled, undifferentiated control; (B) MSC-unlabeled adipogenic changes (magnification × 20); (C) MSC-labeled adipogenic changes (magnification ×20); (D) glycosaminoglycans in unlabeled MSCs (stained red, magnification ×40); (E) glycosaminoglycans in labeled MSCs (stained red, magnification ×40). Undifferentiated FE-Pro-labeled MSCs can be found in Fig. 1(D)

the iron oxide-loaded endosomes fused with lysosomes and at a pH of 4.5 maintained with appropriate buffers resulted in the dissolution of the iron oxide nanoparticles (27). This observation suggests that iron from the nanoparticles can be released into the intracellular compartment and participate in cellular iron metabolism.

Under physiological conditions, increases in intracellular iron trigger an up-regulation of ferritin and down-regulation of transferrin receptor (25). Ferritin and transferrin receptor levels are exquisitely controlled by intracellular iron pools that regulate proteins involved in iron metabolism at the post-transcriptional level (25). Of note, in FE-Pro-labeled cells the iron content can be from 10 to >100 times greater than in unlabeled cells with the iron localized in endosomes. In the current study, a transient decrease in the transferrin receptor gene and in protein expression was observed in both HeLa and MSCs after FE-Pro labeling, possibly in response to the cells detecting the presence of a large increase in intracellular iron in endosomes that would be digested following fusion with lysosomes. In contrast, primary macrophages, which are professional phagocytic cells, showed no changes in TfR-1 protein levels, but increased levels of TfR-1 gene expression. This observation may suggest that professional phagocytes respond differently to increased amounts of intracellular iron released from dissolved ferumoxides. Macrophages may not need to down-regulate TfR-1 owing to their increased cellular

metabolism or their ability to excrete excess of iron back into extracellular space, which is reflected in their decreased iron with time, as presented in Table 3.

Analysis of ferritin expression demonstrated significant increases in both gene and protein expression of ferritin in rapidly dividing FE-Pro-labeled HeLa cells and non-dividing macrophages, but almost constant elevated levels of ferritin were maintained over a period of at least 1 month in FE-Pro-labeled MSCs grown to confluence. The return to control levels of ferritin protein expression in rapidly dividing HeLa versus slowly dividing MSCs can be explained by the possible recirculation of iron back to the extracellular space or by dilution secondary to rapid cell division.

When FE-Pro-labeled MSCs were allowed to divide over time to mimic slow growth *in vivo*, ferritin protein expression returned to unlabeled cell levels within 9 weeks whereas TfR-1 protein expression was not significantly changed due to labeling of cells with FE-Pro. These results suggest that FE-Pro-labeled stem cells may clear the increased iron load through cell division. With each subsequent generation of daughter stem cells or differentiated cells, cellular iron metabolism and storage is regulated in a similar manner to unlabeled stem cells.

Iron in its ferrous state is a component of several metalloproteins that play a crucial role in vital biological processes (22). On the other hand, ferrous ions can be detrimental to the cells. An increase in free intracellular ferrous iron is known to cause production of reactive oxygen species (ROS) through Harber–Weiss–Fenton reactions, which ultimately can result in lipid peroxidation and DNA damage (22). The results of this study confirm previous reports (7,20) that FE-Pro labeling caused no short- or long-term effects on cell viability, proliferation, ROS production or differentiation.

The current study indicates that despite the large amount of iron content introduced into labeled cells, there is no uncoupling of the transferrin and ferritin regulatory metabolic processes. This study provides further evidence supporting the lack of toxicity of labeling cells with ferumoxides and that cellular iron metabolic pathways can process the increase in intracellular iron load. Naturally occurring ferritin in cells is a source of intrinsic MRI contrast in various tissues contributing to the T_1- and T_2-weighted contrast variations in tissues such as brain parenchyma (35). Based on this property of ferritin, two recent reports visualized transgene expression *in vivo* using MRI after transducing cells with ferritin (36,37). The dissolution of ferumoxides in the endosome/lysosome compartment, seen in our studies, should increase ferritin levels within slowly replicating or differentiated cells resulting in a continued shortening of T_2 and T_2^* of the cells in the tissue and a persistent decrease in signal intensity in areas containing labeled cells.

The methods used in this study may serve as general guidelines for future evaluation of new superparamagnetic iron oxide nanoparticles that may be used for cell labeling studies or as targeted MR contrast. The results clearly show that iron oxide-labeled cells can handle iron overload and therefore survive *in vivo* for an extended periods of time. Furthermore, the results indicate that any release of iron, potentially due to cell death or other causes, will not result in iron accumulation, but should be cleared by macrophages, which have efficient and distinct mechanisms of iron metabolism and clearance. The potential clinical implications would suggest that magnetically labeled stem cells that differentiate following limited numbers of cell division may be detected by *in vivo* MRI for prolonged periods of time due to iron oxide nanoparticles in endosomes or iron stored safely in ferritin.

Acknowledgements

This research was supported by the Intramural Research Program of the Clinical Center in the National Institutes of Health.

REFERENCES

1. Ferrucci JT, Stark DD. Iron oxide-enhanced MR imaging of the liver and spleen: review of the first 5 years. *AJR Am. J. Roentgenol.* 1990; **155**: 943–950.
2. Pouliquen D, Le Jeune JJ, Perdrisot R, Ermias A, Jallet P. Iron oxide nanoparticles for use as an MRI contrast agent: pharmacokinetics and metabolism. *Magn. Reson. Imaging* 1991; **9**: 275–283.
3. Yeh TC, Zhang W, Ildstad ST, Ho C. *In vivo* dynamic MRI tracking of rat T-cells labeled with superparamagnetic iron-oxide particles. *Magn. Reson. Med.* 1995; **33**: 200–208.
4. Kaufman CL, Williams M, Ryle LM, Smith TL, Tanner M, Ho C. Superparamagnetic iron oxide particles transactivator protein-fluorescein isothiocyanate particle labeling for *in vivo* magnetic resonance imaging detection of cell migration: uptake and durability. *Transplantation* 2003; **76**: 1043–1046.
5. Frank JA, Anderson SA, Kalsih H, Jordan EK, Lewis BK, Yocum GT, Arbab AS. Methods for magnetically labeling stem and other cells for detection by *in vivo* magnetic resonance imaging. *Cytotherapy* 2004; **6**: 621–625.
6. Hoehn M, Kustermann E, Blunk J, Wiedermann D, Trapp T, Wecker S, Focking M, Arnold H, Hescheler J, Fleischmann BK, Schwindt W, Buhrle C. Monitoring of implanted stem cell migration *in vivo*: a highly resolved *in vivo* magnetic resonance imaging investigation of experimental stroke in rat. *Proc. Natl. Acad. Sci. USA* 2002; **99**: 16267–16272.
7. Arbab AS, Yocum GT, Kalish H, Jordan EK, Anderson SA, Khakoo AY, Read EJ, Frank JA. Efficient magnetic cell labeling with protamine sulfate complexed to ferumoxides for cellular MRI. *Blood* 2004; **104**: 1217–1223.
8. Anderson SA, Glod J, Arbab AS, Noel M, Ashari P, Fine HA, Frank JA. Noninvasive MR imaging of magnetically labeled stem cells to directly identify neovasculature in a glioma model. *Blood* 2005; **105**: 420–425.
9. Daldrup-Link HE, Rudelius M, Oostendorp RA, Jacobs VR, Simon GH, Gooding C, Rummeny EJ. Comparison of iron oxide labeling properties of hematopoietic progenitor cells from umbilical cord blood and from peripheral blood for subsequent *in vivo* tracking in a xenotransplant mouse model XXX. *Acad. Radiol.* 2005; **12**: 502–510.
10. Dardzinski BJ, Schmithorst VJ, Holland SK, Boivin GP, Imagawa T, Watanabe S, Lewis JM, Hirsch R. MR imaging of murine

arthritis using ultrasmall superparamagnetic iron oxide particles. *Magn. Reson. Imaging* 2001; **19**: 1209–1216.
11. Anderson SA, Shukaliak-Quandt J, Jordan EK, Arbab AS, Martin R, McFarland H, Frank JA. Magnetic resonance imaging of labeled T-cells in a mouse model of multiple sclerosis. *Ann. Neurol.* 2004; **55**: 654–659.
12. Weissleder R, Stark DD, Engelstad BL, Bacon BR, Compton CC, White DL, Jacobs P, Lewis J. Superparamagnetic iron oxide: pharmacokinetics and toxicity. *AJR Am. J. Roentgenol.* 1989; **152**: 167–173.
13. Josephson L, Tung CH, Moore A, Weissleder R. High-efficiency intracellular magnetic labeling with novel superparamagnetic-Tat peptide conjugates. *Bioconjug. Chem.* 1999; **10**: 186–191.
14. Lewin M, Carlesso N, Tung CH, Tang XW, Cory D, Scadden DT, Weissleder R. Tat peptide-derivatized magnetic nanoparticles allow *in vivo* tracking and recovery of progenitor cells. *Nat. Biotechnol.* 2000; **18**: 410–414.
15. Frank JA, Zywicke H, Jordan EK, Mitchell J, Lewis BK, Miller B, Bryant LH, Jr., Bulte JW. Magnetic intracellular labeling of mammalian cells by combining (FDA-approved) superparamagnetic iron oxide MR contrast agents and commonly used transfection agents. *Acad. Radiol.* 2002; **9**(Suppl. 2): S484–S487.
16. Frank JA, Miller BR, Arbab AS, Zywicke HA, Jordan EK, Lewis BK, Bryant LH, Jr., Bulte JW. Clinically applicable labeling of mammalian and stem cells by combining superparamagnetic iron oxides and transfection agents. *Radiology* 2003; **228**: 480–487.
17. Hill JM, Dick AJ, Raman VK, Thompson RB, Yu ZX, Hinds KA, Pessanha BS, Guttman MA, Varney TR, Martin BJ, Dunbar CE, McVeigh ER, Lederman RJ. Serial cardiac magnetic resonance imaging of injected mesenchymal stem cells. *Circulation* 2003; **108**: 1009–1014.
18. Daldrup-Link HE, Rudelius M, Oostendorp RA, Settles M, Piontek G, Metz S, Rosenbrock H, Keller U, Heinzmann U, Rummeny EJ, Schlegel J, Link TM. Targeting of hematopoietic progenitor cells with MR contrast agents. *Radiology* 2003; **228**: 760–767.
19. Kalish H, Arbab AS, Miller BR, Lewis BK, Zywicke HA, Bulte JW, Bryant LH, Jr., Frank JA. Combination of transfection agents and magnetic resonance contrast agents for cellular imaging: relationship between relaxivities, electrostatic forces, and chemical composition. *Magn. Reson. Med.* 2003; **50**: 275–282.
20. Arbab AS, Yocum GT, Kalish H, Jordan EK, Anderson SA, Khakoo AY, Read EJ, Frank JA. Response to Letter to the Editor, re ferumoxides-protamine sulfate labeling does not alter differentiation of mysenchymal stem cells. *Blood* 2004; **104**: 3412–3413.
21. Moore A, Basilion JP, Chiocca EA, Weissleder R. Measuring transferrin receptor gene expression by NMR imaging. *Biochim. Biophys. Acta* 1998; **1402**: 239–249.
22. Papanikolaou G, Pantopoulos K. Iron metabolism and toxicity. *Toxicol. Appl. Pharmacol.* 2005; **202**: 199–211.
23. Crichton RR, Wilmet S, Legssyer R, Ward RJ. Molecular and cellular mechanisms of iron homeostasis and toxicity in mammalian cells. *J. Inorg. Biochem.* 2002; **91**: 9–18.
24. Crichton RR, Ward RJ. An overview of iron metabolism: molecular and cellular criteria for the selection of iron chelators. *Curr. Med. Chem.* 2003; **10**: 997–1004.
25. Aisen P, Enns C, Wessling-Resnick M. Chemistry and biology of eukaryotic iron metabolism. *Int. J. Biochem. Cell Biol.* 2001; **33**: 940–959.
26. Arbab AS, Bashaw LA, Miller BR, Jordan EK, Lewis BK, Kalish H, Frank JA. Characterization of biophysical and metabolic properties of cells labeled with superparamagnetic iron oxide nanoparticles and transfection agent for cellular MR imaging. *Radiology* 2003; **229**: 838–846.
27. Arbab AS, Wilson LB, Ashari P, Jordan EK, Lewis BK, Frank JA. A model of lysosomal metabolism of dextran coated superparamagnetic iron oxide (SPIO) nanoparticles: implications for cellular magnetic resonance imaging. *NMR Biomed.* 2005; **18**: 383–389.
28. Laemmli UK. Cleavage of structural proteins during the assembly of the head of bacteriophage T4. *Nature* 1970; **227**: 680–685.
29. Mosmann T. Rapid colorimetric assay for cellular growth and survival: application to proliferation and cytotoxicity assays. *J. Immunol. Methods* 1983; **65**: 55–63.
30. Hansen MB, Nielsen SE, Berg K. Re-examination and further development of a precise and rapid dye method for measuring cell growth/cell kill. *J. Immunol. Methods* 1989; **119**: 203–210.
31. Berridge MV, Tan AS. Characterization of the cellular reduction of 3-(4,5-dimethylthiazol-2-yl)-2,5-diphenyltetrazolium bromide (MTT): subcellular localization, substrate dependence, and involvement of mitochondrial electron transport in MTT reduction. *Arch. Biochem. Biophys.* 1993; **303**: 474–482.
32. Arbab AS, Yocum GT, Rad AM, Khakoo AY, Fellowes V, Read EJ, Frank JA. Labeling of cells with ferumoxides-protamine sulfate complexes does not inhibit function or differentiation capacity of hematopoietic or mesenchymal stem cells. *NMR Biomed.* 2005; **18**: 553–559.
33. Bulte JW, Miller GF, Vymazal J, Brooks RA, Frank JA. Hepatic hemosiderosis in non-human primates: quantification of liver iron using different field strengths. *Magn. Reson. Med.* 1997; **37**: 530–536.
34. Bulte JW, Douglas T, Witwer B, Zhang SC, Strable E, Lewis BK, Zywicke H, Miller B, van Gelderen P, Moskowitz BM, Duncan ID, Frank JA. Magnetodendrimers allow endosomal magnetic labeling and *in vivo* tracking of stem cells. *Nat. Biotechnol.* 2001; **19**: 1141–1147.
35. Vymazal J, Zak O, Bulte JW, Aisen P, Brooks RA. T1 and T2 of ferritin solutions: effect of loading factor. *Magn. Reson. Med.* 1996; **36**: 61–65.
36. Cohen B, Dafni H, Meir G, Harmelin A, Neeman M. Ferritin as an endogenous MRI reporter for noninvasive imaging of gene expression in C6 glioma tumors. *Neoplasia* 2005; **7**: 109–117.
37. Genove G, DeMarco U, Xu H, Goins WF, Ahrens ET. A new transgene reporter for *in vivo* magnetic resonance imaging. *Nat. Med.* 2005; **11**: 450–454.